Powder Diffraction

Direct Localization of Atoms in Mixed-Occupancy Powders by Resonant Contrast Diffraction

Herve Palancher, Jean-Louis Hodeau, Christophe Pichon, Jean-François Bérar, John Lynch, Bernadette Rebours, and Juan Rodriguez-Carvajal*

Presently, one challenge in structural determination is to describe the detailed atomic order in complex powders such as natural samples or materials involved in industrial processes (cement manufacturing, production of chemicals, mineral extraction). Classical X-ray powder diffraction is a key technique for this investigation but it has intrinsic limitations, especially the difficulty in discriminating between elements with similar atomic numbers or occupying neighboring sites.

In the study of complex samples (structures with large cell parameters), an "acceptable" fit can correspond to a false local minimum, with inappropriate attribution of electron density to a given element compensated by an inaccurate localization or quantification of other atoms in the unit cell. A common and difficult problem in powdered samples is the detailed study of mixed powders (with either several phases or a range of atomic occupancies in the same phase), as occurs in minerals and in industrial preparations. Furthermore, chemical or physical properties are generally driven (or at least affected) by the localization of some specific atoms in a mixture.

Two different methods are used to enhance the chemical contrast between elements in powder diffraction techniques. The first one uses neutron diffraction, since the nuclear scattering length is not related to the atomic number. The efficiency of this technique for contrast studies is, in general, satisfactory, but it requires large samples, and the high resolution obtained with synchrotron radiation cannot be achieved in current neutron diffractometers. This last point is primordial for powder diffraction, where reflections may overlap on the one-dimensional diffraction pattern. The second method uses resonant X-ray diffraction. The variation of the resonant scattering contribution near the edge of a given atom affects the contribution of this specific atom to the diffracted intensities.[1] Based on this effect, a site-selective technique, namely diffraction anomalous fine structure (DAFS) has been developed that combines diffraction and spectroscopic measurements.[2–5] Moreover, the anomalous effect provides an elegant and efficient way of solving the structure factor phase problem in bio-crystallography by the so-called multiwavelength anomalous diffraction (MAD)[6–8] and single-wavelength anomalous diffraction (SAD) methods.[9,10] The software and the experimental developments dedicated to these studies, as well as the worldwide availability of synchrotron radiation, have made this a well-established method that is routinely used by structural biologists.[11] A third type of application uses the chemical sensitivity of resonant diffraction to extract the contribution of a single element in a given crystallographic site and this resonant contrast diffraction (RCD) is the focus of the present contribution.

The specificities of the RCD method were demonstrated on powders in the 1990s.[12–15] Thanks to partial Patterson density maps and maximum entropy methods (MEMs) it was possible to use resonant diffraction for ab initio structure determination.[16] However, this ab initio structure solution method can become inefficient for complex powder samples due to the small number of non-overlapping reflections, and direct space methods such as those based on genetic algorithms and simulated annealing[17] are generally used to solve the structure of organic samples of high interest for the pharmaceutical industry.[18] It has been shown that differential anomalous scattering and partial structure factor analysis are efficient for studying amorphous-like materials such as glasses, liquids, nanoparticles, and also crystallized catalysts.[19,20] They have also been used for quantitative analysis of minority phases such as Pt-metal inclusions in amorphous or crystalline substrates. Nevertheless, this resonant technique is still not widely used in powder diffraction, probably due to its relative complexity. Herein, we make use of recent advances in both MAD methods used in bio-crystallography and DAFS methods used for site-selective spectroscopy to show that accurate localization of atoms in powders is possible by the routine use of "anomalous differential patterns". The gain in the multi-wavelength powder data refinement allows a direct visualization of these atoms by "dispersive difference maps".

Owing to the superposition of (hkl) and $(-h-k-l)$ reflections in powder diffraction diagrams, the SAD method (based on f'' variation and calculations of Bijvoet difference maps) cannot be used. In powder diffraction, the intensity difference is mainly a function of $\Delta f'$ ($\Delta f'$ is the difference between the two f' values for the same resonant element at the two data collection energies) and can allow the calculation of "dispersive difference maps", as performed currently by bio-crystallographers: the scattering contrast for a defined element is obtained by collecting data at two different photon energies. The Bragg intensities in powder diffraction data are much weaker than in single-crystal studies, and the relative weakness of the anomalous f' and f'' contribution (-8 to -5 electron unit (eu) for transition metals) compels us to collect patterns with very good statistics and to eliminate systematic errors.

[*] H. Palancher, Dr. J.-L. Hodeau, Dr. J.-F. Bérar
Laboratoire de Cristallographie (CNRS)
25, avenue des Martyrs, 38042 Grenoble Cedex (France)
Fax: (+33) 4-7688-1038
E-mail: hodeau@grenoble.cnrs.fr
H. Palancher, Dr. C. Pichon, Dr. J. Lynch, B. Rebours
Institut Français du Pétrole
BP3, 69390 Vernaison (France)
Dr. J.-F. Bérar
French CRG BM2 - ESRF
6, rue Jules Horowitz, 38049 Grenoble Cedex 9 (France)
Dr. J. Rodriguez-Carvajal
Laboratoire Léon Brillouin (CEA-CNRS)
CEA/Saclay
91191 Gif/Yvette (France)

 DOI: 10.1002/ange.200461642

Herein, this multiwavelength approach using resonant scattering is developed and validated by the analysis of a well-crystallized solid of industrial interest: hydrated SrRbX zeolite.[21] This sample, in which both Sr^{2+} and Rb^{+} ions have the same number of electrons ($Z = 36$ eu), is a particularly difficult case for conventional X-ray diffraction. Neutron diffraction is also unable to discriminate between the two nuclei because their scattering lengths are too close: $b(\mathrm{Sr}) = 0.702 \times 10^{-14}$ m and $b(\mathrm{Rb}) = 0.709 \times 10^{-14}$ m. In X-type zeolites the cations compensate the negatively charged framework. In a first step, SrX was prepared by aqueous ion-exchange from NaX.[22] The dicationic SrRbX sample was then obtained from SrX by the same chemical process. Its composition ($Sr_{24}Rb_{15}Na_4\ Al_{79}Si_{113}O_{384}{\cdot}211\,H_2O$) was determined by elemental and thermogravimetric analyses. Diffraction measurements were performed on the BM2 beamline at the European Synchrotron Radiation Facility (ESRF).

To validate our methodology, diffraction patterns with a $s = 1/d = 2\,sin\theta/\lambda$ range up to at least 1.0 $Å^{-1}$, were collected in Debye–Scherrer geometry on the hydrated SrRbX sample at

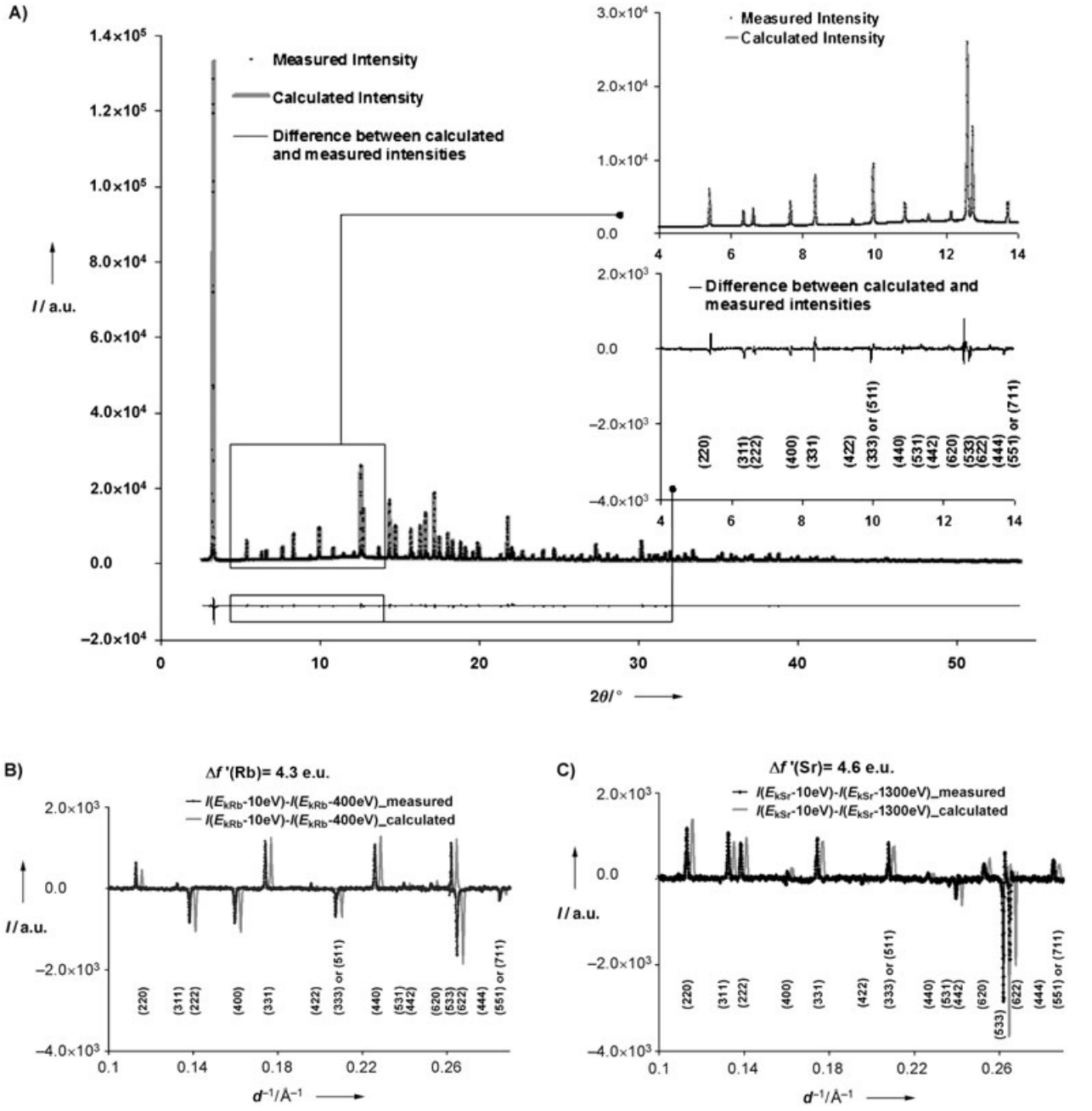

Figure 1. Influence of anomalous effects at the strontium and rubidium edges on the intensity of various reflections of diffraction patterns collected for hydrated SrRbX: A) Measured diffraction data and calculated diagram recorded for a hydrated SrRbX sample at E_{KSr} −1300 eV; insert: zoom of diffracted and conventional difference diagram for $0.10\ Å^{-1} < 1/d < 0.29\ Å^{-1}$. B) Comparison of the measured and calculated "anomalous differential patterns" at the rubidium K absorption edge (difference between diagrams obtained at E_{KSr} −10 eV and E_{KSr} −1300 eV). The calculated pattern is shifted along the *x* axis for better visualization of the intensity variations, C) Same figure as (B) but performed at the strontium K absorption edge. For (B) and (C) the same intensity normalization was applied.[34]

three energies: about 10 eV below the rubidium and the strontium K absorption edges ($E_{KRb}=15.192$ and $E_{KSr}=16.096$ keV, respectively) and at 14.800 keV, far below both edges. Figure 1 A shows the diffraction pattern collected at E_{KSr} −1300 eV. The high quality of the diffraction patterns enables the observation of intensity variations with energies exceeding the background noise. The anomalous effect can be clearly seen in the two anomalous difference patterns calculated from data collected at E_{KSr} −10 eV and E_{KSr} −1300 eV at the strontium absorption edge (and at E_{KRb} −10 eV and E_{KRb} −400 eV at the rubidium absorption edge), so that they can be taken into account in the pattern refinement (Figure 1B, C).

This data set has been refined with FULLPROF, a multipattern profile refinement software that uses the Rietveld method.[23,24] As it is very often the case in industrial or mineral compounds, where the framework structure is roughly known, we do not need ab initio methods: in X-type zeolites we can introduce the basic framework atomic positions in the refinement. The initial relative intensities of the different peaks that contribute to overlapped reflections, and the rough initial phases determined by these positions, allow us to calculate an initial Fourier map from the amplitude of the "observed" structure factors and the calculated phases. These Fourier maps are proportional to the electron density of the structure and already give a rough and non-element-selective localization of all extra-framework atoms (cations, molecules such as water, etc.). In X-type zeolites the cations and water are normally located at the well-known sites I, I′, II, II′, and III (Figure 2 A). However, they can be introduced in the refinement only as electron densities, with no assumption of the atom type. Figure 2 B shows the electron density calculated for the hydrated SrRbX sample in a plane (hereafter labelled *P*) containing the two ⟨111⟩ axes shown schematically in Figure 2 A. The occupancies of the different atoms (cations, water) are normally differentiated only by a chemical knowledge of the usual atom-to-framework distances. By using resonant diffraction

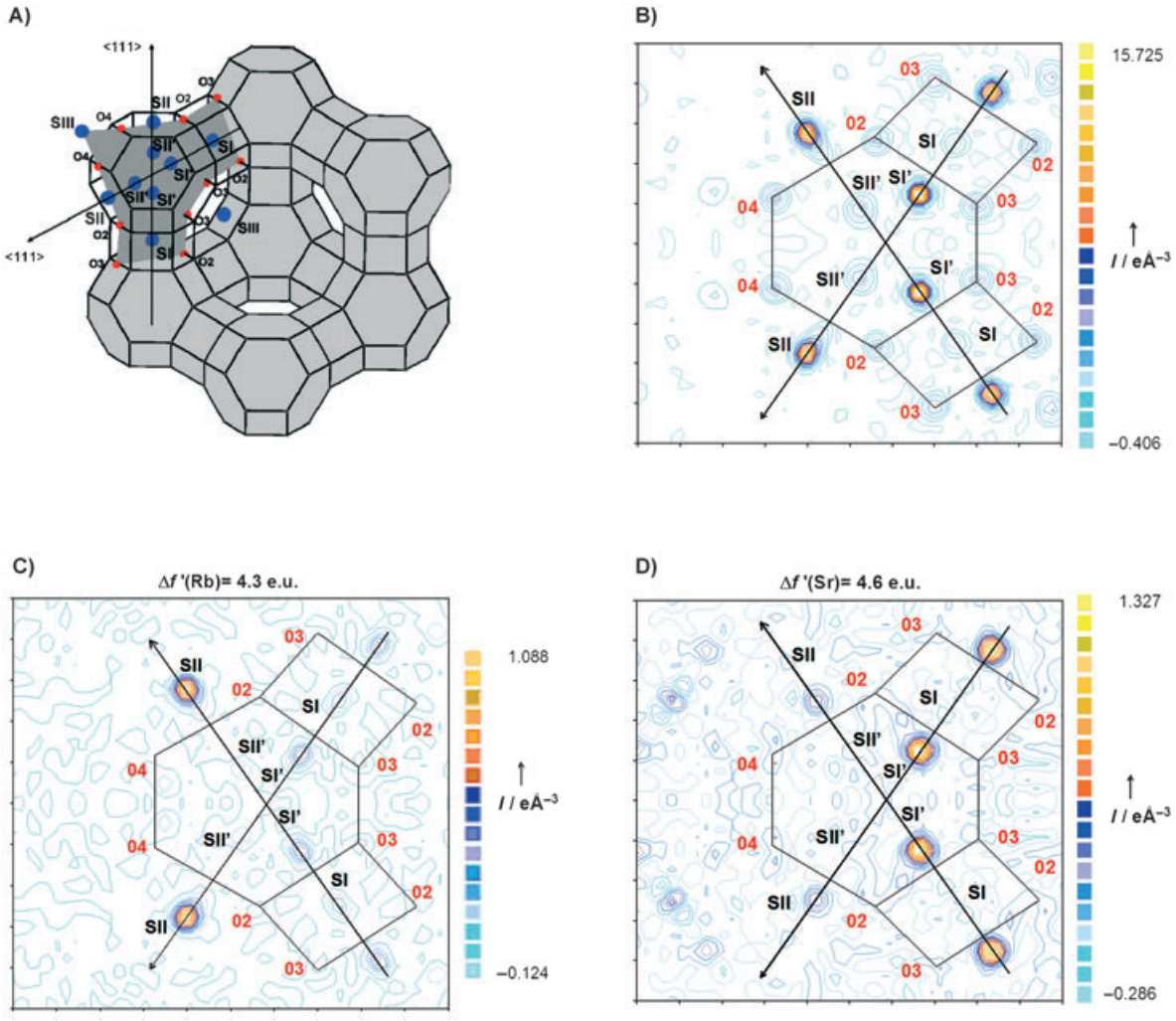

Figure 2. Strontium and rubidium cation localization in a water-saturated SrRbX sample: A) Localization of the main cationic sites in the unit cell of X-type zeolite. Sites I, I′, II′, II, and III are labeled SI, SI′, SII′, SII, and SIII, respectively. Plane *P*, defined by the intersection of two <111> axes, is represented in dark gray. B) Fourier map in the *P* plane calculated from diffraction data measured at $E_{KSr}=-1300$ eV. Electronic densities appear at sites I, I′, II′, and II. C) Dispersive difference electron-density maps calculated at the rubidium K absorption edge ($\Delta f'$(Rb) = 4.3 e.u.). D) Same figure as (C) but performed at the strontium K absorption edge ($\Delta f'$(Sr) = 4.6 e.u.). Electronic density at site II′ cannot be attributed to rubidium or strontium cations.

at the edge of one of these atoms, we can calculate the difference between the electron densities determined from patterns collected at various energies. This corresponds to Fourier maps ("dispersive difference maps") in which the amplitude of the Fourier coefficients is proportional to the difference of the structure factors of both energies, so that the corresponding density is proportional to the variation of the real anomalous term of the resonant scatterers ($\Delta f'$) (this has been confirmed by an RCD study of a hydrated SrX sample at the Sr^{2+} K absorption edge).[25] "Dispersive difference maps" (P plane) have been obtained at both the Rb^+ and Sr^{2+} absorption edges on hydrated SrRbX (Figure 2C,D): no noticeable intensity appears at the localization of the framework atoms. These results show that the use of "dispersive difference maps" enables not only resonant cation localization but also their quantification.

It is obvious that accurate values for the anomalous scattering factors f' and f'' are needed. For each data collection energy, values for the cation anomalous terms f' and f'' were determined experimentally. At energies far from the absorption edges of the considered element they are not influenced by the chemical environment; tabulated values for the free atoms are therefore satisfactory.[26] For energies close to an absorption edge, the f' and f'' values have to be determined directly for the sample studied since absorption edge displacements due to valence variations and fine-structure oscillations can strongly modify their values. When performing diffraction measurements, the easiest method consists in collecting absorption spectra in fluorescence or transmission mode. Values for f' and f'' can then be obtained with the Kramers–Kronig relationship.[27] As shown in Figure 3, corrections of f' and f'' values close to the absorption edge may reach 10%, and accuracy is directly related to the quality of the experimental determination of f' and f''.

Both types of information (cation localization and anomalous scattering factors) were introduced into a structural model, thereby enabling the calculation of diffraction diagrams at $E_{K\,Sr}$ −10 eV and at $E_{K\,Rb}$ −10 eV. A comparison of the calculated and measured "anomalous differential patterns" at both the rubidium and strontium absorption edges shows a close agreement between the two (Figure 1B,C). Such "anomalous difference patterns" are extremely sensitive to resonant atom location and occupancy, and are a key agreement test for various atom occupancies in sites occupied by chemically different cations.[28]

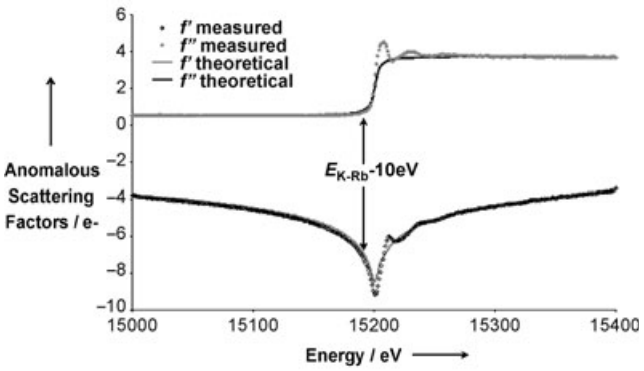

Figure 3. Rubidium f' and f'' values determined as a function of energy by using the Kramers–Kronig transformation of strontium K absorption data measured on a hydrated SrX sample in transmission mode.

The high resolution of our data collection enables a mixed population of site II to be detected in the initial Fourier map derived from the data collected at $E_{K\,Sr}$ −1300 eV (Figure 2B) from the weak splitting of the peak at site II. Each extra framework species (Sr^{2+}, Rb^+, Na^+, H_2O) has a given radius and its position depends on the bond length between the cations and the oxygen atoms of the framework. Here also the occupancies of the different atoms corresponding to such a splitting can be determined independently by the use of "dispersive difference maps" obtained at both the Rb^+ and Sr^{2+} absorption edges (Figure 2C,D). It appears that Sr^{2+} ions occupy sites I′ and II, whereas Rb^+ ions are located mainly at site II but also at sites I and I′. The presence of both cations at sites II and I′ is thus proven and can be directly seen in these differential electron-density maps.

The accuracy of this methodology can also be illustrated by a study of the population in sites I and II′. Classical refinement of the diffraction patterns of the hydrated SrRbX sample leads to identical results irrespective of whether these sites are considered as being occupied solely by residual, non-exchanged sodium cations or by a combination of sodium and rubidium cations. The difference anomalous Fourier map at the rubidium edge simulated for both site I occupation possibilities confirms the presence of Rb^+ cations at this site. Moreover, using the same strategy, anomalous diffraction at the rubidium K absorption edge shows the unique presence of water molecules in site II′ (Figure 2C).[29]

Based on the experimental improvement of data collection achieved with DAFS spectroscopy and applied by using the MAD principles, a methodology has been developed for powder-sample analysis that optimizes the use and the interpretation of anomalous information. Our aim was to validate, using a real-world example, the resonant scattering method for contrast studies in complex powders with mixed-occupancy sites. We have shown that, even in powder samples with considerable reflection overlap and with a basically known framework, the use of "dispersive difference" electron density maps allows an easy localization of the resonant atoms. The use of "anomalous difference patterns" enables good agreement factors to be achieved for accurate localization. These two specific difference tools can also be used with powders containing several phases. The application of these methods can be extended to numerous materials in geology, industry, and environmental studies to localize transition metals or heavy atoms. It can also give their valence by the use of diffraction anomalous near-edge structure (DANES) spectroscopy[3,5,30] with powders; that is, refinement of the f' value to extract the chemical shift in the resonant-atom absorption edge. The extension of resonant contrast diffraction to measurements in situ can also be foreseen for the analysis of the evolution of atomic order during chemical reactions.

Received: August 13, 2004
Published online: February 11, 2005

Keywords: anomalous scattering · cation distribution · powder diffraction · resonant contrast diffraction · structure elucidation · zeolites

[1] For X-ray diffraction, the expression for the atomic scattering factor, f, consists of three terms: $f = f_0 + f' + if''$, where f_0 defines classical Thomson scattering, and the resonant (or anomalous) f' and f'' represent dispersion and absorption processes, respectively. Their values vary strongly with energy when the incoming photon energy is close to an absorption edge. The structure factor F_{hkl} is derived from the atomic scattering factors of the elements constituting the unit cell weighted by their localization in the cell. Therefore, since the diffracted intensity is proportional to $|F_{(hkl)}|^2$, it also depends on the resonant scattering factors of the elements.

[2] H. Stragier, J. O. Cross, J. J. Rehr, L. B. Sorensen, C. E. Bouldin, J. C. Woicik, *Phys. Rev. Lett.* **1992**, *69*, 3064 – 3067.

[3] I. J. Pickering, M. Sansone, J. Marsch, G. N. George, *J. Am. Chem. Soc.* **1993**, *115*, 6302 – 6311.

[4] L. B. Sorensen, J. O. Cross, M. Newville, B. Ravel, J. J. Rehr, H. Stragier, C. E. Bouldin, J. C. Woicik, in *Resonant Anomalous Diffraction X-ray Scattering* (Eds.: G. Materlik, C. J. Sparks, K. Fischer), Elsevier Science B.V., Amsterdam, **1994**, pp. 389 – 420.

[5] J. L. Hodeau, V. Favre-Nicolin, S. Bos, H. Renevier, E. Lorenzo, J. F. Berar, *Chem. Rev.* **2001**, *101*, 1843 – 1867.

[6] In the MAD method, the variation of intensity reflections with energy, caused by the energy fluctuation of anomalous scattering factors, is interpreted to locate the anomalous scatterers.

[7] W. A. Hendrickson, M. M. Teeter, *Nature* **1981**, *290*, 107 – 113.

[8] W. A. Hendrickson, *Science* **1991**, *254*, 51 – 58.

[9] The SAD method is based on the study of intensity differences for $(h\,k\,l)$ and $(-h\,-k\,-l)$ reflections at a given energy due to the contribution of anomalous scattering factors.

[10] J. M. Bijvoet, *Proc. Acad. Sci. Amsterdam B* **1949**, *52*, 313 – 314.

[11] CCP4: *Acta Crystallogr. Sect. D* **1994**, *50*, 760 – 763.

[12] R. S. Howland, T. H. Geballe, S. S. Laderman, A. Fischer-Colbrie, M. Scott, J. M. Tarascon, P. Barboux, *Phys. Rev. B* **1989**, *39*, 9017 – 9027.

[13] J. P. Attfield, *Nature* **1990**, *343*, 46 – 49.

[14] G. H. Kwei, R. B. Von Dreele, A. Williams, J. A. Goldstone, A. C. Lawson II, W. K. Warburton, *J. Mol. Struct.* **1990**, *223*, 383 – 406.

[15] D. E. Cox, A. P. Wilkinson in *Resonant Anomalous Diffraction X-ray Scattering* (Eds.: G. Materlik, C. J. Sparks, K. Fischer), Elsevier Science B.V., Amsterdam, **1994**, pp. 195 – 219.

[16] K. Burger, D. Cox, R. Papoular, W. Prandl, *J. Appl. Crystallogr.* **1998**, *31*, 789 – 797.

[17] For a review see: K. D. M. Harris, M. Tremayne, B. M. Kariuki, *Angew. Chem.* **2001**, *113*, 1674 – 1700; *Angew. Chem. Int. Ed.* **2001**, *40*, 1626 – 1651.

[18] S. Pagola, P. W. Stephens, D. S. Bohle, A. D. Kosar, S. K. Madsen, *Nature* **2000**, *404*, 307 – 310.

[19] E. Matsubara, Y. Waseda, in *Resonant Anomalous Diffraction X-ray Scattering* (Eds.: G. Materlik, C. J. Sparks, K. Fischer), Elsevier Science B.V., Amsterdam, **1994**, pp. 345 – 364.

[20] C. Meneghini, S. Mobilio, L. Lusvarghi, F. Bondioli, A. M. Ferrari, T. Manfredini, C. Siligardi, *J. Appl. Crystallogr.* **2004**, *37*, 890 – 900.

[21] SrRbX stands for zeolite NaX highly exchanged with Sr^{2+} and Rb^+ cations.

[22] This sample was prepared by aqueous ion-exchange at 353 K from a NaX zeolite and a 1 mol L^{-1} solution of $Sr(NO_3)_2$.[31] After activation at 573 K under nitrogen flow the sample was slowly rehydrated.

[23] H. M. Rietveld, *J. Appl. Crystallogr.* **1969**, *2*, 65 – 71.

[24] J. Rodríguez-Carvajal, *Physica B* **1993**, *192*, 55 – 69. For a recent version see: Juan Rodríguez-Carvajal, *Recent Developments of the Program FULLPROF* in, Commission on Powder Diffraction (IUCr), Newsletter **2001**, *26*, 12 – 19, available at http://journals.iucr.org/iucr-top/comm/cpd/Newsletters/. The complete program and documentation can be obtained from the anonymous ftp-site: ftp://ftp.cea.fr/pub/llb/divers/fullprof.2k.

[25] Powder-diffraction measurements were performed with a hydrated SrX sample following the same strategy (as detailed for SrRbX in the text) at three energies: 16.196 keV (E_{KSr} −10 eV), 16.041 keV (E_{KSr} −65 eV), and 15.192 keV (E_{KSr} −904 eV). At the Sr^{2+} absorption edge, two "dispersive difference" maps were calculated from diagrams collected at E_{KSr} −904 eV and E_{KSr} −65 eV (for the first), and at E_{KSr} −904 eV and E_{KSr} −10 eV in the second case. The maximum intensities on these maps obtained for sites I′ and II are 0.775/1.421 and 0.664/1.217, respectively, with energy variations corresponding to $\Delta f' = 2.6$ e.u./4.8 e.u.

[26] For calculated values, see, for example: S. Sasaki, *Anomalous Scattering Factors for Synchrotron Radiation Users Calculated Using Cromer Liberman's method*, National Laboratory for High-Energy Physics, Tsukuba (Japan), **1984**.

[27] f' and f'' are linked by the Kramers–Kronig relationships: $f'\omega_0 = \frac{2}{\pi}P\int_0^\infty \frac{\omega f''(\omega_0)}{\omega^2-\omega_0^2}d\omega$ and $f''\omega_0 = \frac{2}{\pi}P\int_0^\infty \frac{\omega f'(\omega_0)}{\omega^2-\omega_0^2}d\omega$. To apply the Kramers–Kronig relationship, f' or f'' must be known over a very large energy range (ranging from ~30 eV up to ~200 keV for an absorption edge near 10 keV). Thus, for such a calculation theoretical values are generally used far from the edge and merged to experimental values. We applied the Kramers–Kronig relationship to the difference spectrum (experimental factor minus the theoretical one), the final resonant factor being the sum of the result and the tabulated theoretical factor.[32,33]

[28] In the current version of FULLPROF (version 2.70) the use of "anomalous differential patterns" and a direct plot of normalized near-edge minus far-from-edge difference patterns is possible.

[29] The distinction between cations and water molecules in zeolites X or Y is of high importance regarding the influence of water molecules in hydrocarbon adsorption processes.

[30] S. Bos, PhD thesis, University of Grenoble (France), **1999**.

[31] H. S. Sherry, *J. Phys. Chem.* **1968**, *72*, 4086 – 4094.

[32] L. K. Templeton, D. H. Templeton, *J. Appl. Crystallogr.* **1988**, *21*, 558 – 561.

[33] G. Evans, R. Pettifer, *J. Appl. Crystallogr.* **2001**, *34*, 82 – 86.

[34] With the $Fd\bar{3}m$ space group, the elements situated on the ⟨111⟩ axis contribute to all reflections. In consequence, no reflection can, in principle, be used for intensity normalization between diagrams collected at different energies below a cation absorption edge. The reflection (1086), which is less sensitive to cations, was chosen as a reference.

